Published in final edited form as:
Biotechniques. 2006 October ; 41(4): 399–402.

Automated single-cell electroporation

Chilman Bae and **Peter J. Butler**
The Pennsylvania State University, University Park, PA, USA

Cells regulate physiological processes through compartmentalization of molecular-scale signaling and through coordinated interaction with neighboring cells. To unravel the complex interplay of these events on these small-length scales, researchers track or selectively modify cell biology at the single-cell and single-molecule levels by inserting foreign molecules (e.g., dyes, drugs, DNA, RNA, proteins, peptides, and amino acids) by microinjection, transfection, chemical modification, or electroporation. Single-cell electroporation (SCE) is an emerging noninvasive technique for cell-specific insertion of small molecules by electro-kinetic force and diffusion across electric field-induced membrane pores at the end of a small electrode. These electrodes are based on micropipets (micropipet electrode; ME) (1), solid carbon fibers (2), electrolyte-filled capillaries (3), or chip-based microfabricated electrode arrays (4).

The ME-based (or patchclamp-based) microelectroporation method is ideal for adherent cells because (*i*) the ME can indent the cell and create membrane tension that lowers the voltage needed for electroporation (5), thus reducing electrically induced cell damage; (*ii*) the volume (often expensive or rare) of inserted molecules is as small as the ME tip (<1.0 μL); and (*iii*) there are no toxic by-products from electrode reactions (6). There are, however, significant impediments to wide-scale use of ME-based SCE. First, it is difficult to manually regulate the approach of the pipet toward the cell using only a microscope or resistance increases arising from pipet contact with the cell membrane (1). Second, SCE efficiency is hampered by variable ME resistances arising from inconsistencies in ME fabrication. Variable ME resistances result in inconsistent applied membrane voltages when ME input voltages are constant, making it difficult to consistently achieve pore-forming transmembrane voltages of 0.2–1.0 V (7–9). Thus, in this study, we developed a new method of ME-based SCE with 40-nm precision feedback control of ME approach and a method to prescribe the applied membrane potential (V_m), a new electrical parameter for increased SCE efficiency.

The three principal design goals for automated SCE (aSCE) were (*i*) image-based cell selection; (*ii*) feedback control of the ME position by real-time measurement of changes in cleft resistance (R_{cl}, see Equation 2); and (*iii*) automation of pulse timing and amplitude. To accomplish these design goals, we integrated a computer-controlled micromanipulator (MP-285; Sutter Instruments, Novato, CA, USA), a high-performance cooled charge-coupled device (CCD) digital imaging camera (Sensicam-ER; Cooke Corporation, Romulus, MI, USA), an A/D board (National Instruments, Austin, TX, USA) (Figure 1B), and a modified current-to-voltage-converting circuit (Figure 1A) with an IX71 microscope (Olympus, Lehigh, PA, USA).

Address correspondence to Peter J. Butler, Department of Bioengineering, The Pennsylvania State University, 228 Hallowell Building, University Park, PA 16802, USA. pbutler@psu.edu.

COMPETING INTERESTS STATEMENT
The authors declare no competing interests.

$$R_e = \left(G \cdot \frac{V_i}{V_{o,ini}} - 1 \right) \cdot R_c \quad \text{[Eq. 1]}$$

$$R_{cl} = \left(G \cdot \frac{V_i}{V_o} - 1 \right) \cdot R_c - R_e \quad \text{[Eq. 2]}$$

$$V_{in}' = V_m \left(\frac{R_e + R_c + R_{cr}}{R_{cr}} \right) \quad \text{[Eq. 3]}$$

A LabVIEW-based software program coordinated ME position, cell imaging, electrical monitoring and pulsing, and data acquisition (Figure 1C).

The phase image of the cell was projected on the computer screen followed by coarse positioning of the ME tip into the field of view. Image-based cell selection was initiated by computer registration of mouse clicks at starting x and y coordinates of the ME tip and destination coordinates of the target cell (Figure 1D). These coordinates defined a vector along which the micromanipulator moved and placed the ME tip directly over the cell to be electroporated. The calibration of distance for a 20× objective was 3.13 pixel/μm.

A circuit was devised by which cleft resistance (R_{cl}) could be used to control and terminate the z-axis approach phase of ME movement toward the target cell (Figure 1A). In the circuit diagram, parameters (R_1, R_2, R_3, R_4, V_i, R_c) were chosen such that the total gain, G, was 470. By measuring the initial output voltage ($V_{o,ini}$), R_e was calculated (Equation 1) and was used to monitor R_{cl} (Equation 2). During the approach and indenting phase, V_i was maintained at 1 V in order to dynamically calculate R_{cl} (Equation 2), which was used for feedback control of pipet approach by the micro-manipulator (0.04 μm/step maximum resolution).

When the ME touched and indented a cell, R_{cl} increased sharply (Figure 2A). The indenting phase of pipet movement was terminated when R_{cl} reached a critical resistance value (R_{cr}) of 0.75 MΩ (determined from control experiments). V_i' was then calculated from Equation 3, using V_m > 0.2 V, and applied as dc square-pulses at the circuit input to initiate electroporation. It is important to note that when the same V_i' is used for all pipets, V_m can be highly variable because R_e varies from pipet to pipet. Our system can accommodate pipets with variable R_e by dynamically adjusting V_i'. Also, when pulses are based on V_m, which is a physiologically relevant pore-forming potential, electroporation efficiency is higher than in experiments where V_i' pulse amplitude does not account for variable R_e (unpublished observations).

To find the optimal V_m and test system repeatability, we used the aSCE system to insert BODIPY® FL-GTP (100 μM, negatively charged; Invitrogen, Carlsbad, CA, USA) into bovine aortic endothelial cells (BAECs) with R_{cr} = 0.75 MΩ, R_e = 10.4 ± 0.41 MΩ, and V_m of 0.2, 0.3, 0.4, 0.5, and 0.67 V. Cells (n > 20) were electroporated one by one using image-based cell selection. The average time for SCE was 40 s/cell. Success rate (when electroporated cell fluorescence intensity was 2 standard deviations above the average intrinsic cell fluorescence intensity) was sharply increased when V_m > 0.3 V; when V_m = 0.4

V, nearly 90% of cells were successively electroporated (Figure 2B). To demonstrate image-based cell selection and assess the relationship between inserted dye and V_m, cells were selected individually as shown in Figure 2C using V_m of 0.3, 0.4, and 0.5 V for cells marked by P, S, and U, respectively. The electroporated-BODIPY FL-GTP intensity increased with increasing V_m suggesting that V_m can be used to ensure and predetermine dye uptake. It is important to note that increases in pulse amplitude increase both membrane pore size (10), number (11), and electrokinetic forces. Because the pipet indents the membrane and seals the tip, most of the voltage drop is across the membrane and nearly equal to V_m. Thus, the ability of V_m of 0.4 V to generate pores large enough for electrokinetic-induced BODIPY FL-GTP dye insertion is consistent with previous studies that demonstrated a pore-inducing transmembrane voltage threshold of 0.2 V (7).

Viability of electroporated cells was also assessed. Using protocols and voltages identical to the previous BODIPY-FL experiments (n = 15 for each voltage), cells were incubated for 2.5 h and then stained with calcein red-orange AM (Invitrogen). In order to assist in finding the cells after the incubation period, small scratches were made on the coverslips using a diamond-tipped marker. We found that nearly all the cells were stained positively with calcein, indicating that cell membranes were intact. Upon visual inspection of the cells under 20× phase microscopy, small vacuoles appeared in about 20% of cells that were electroporated with V_m = 0.67 V. V_m of 0.5 V or less did not induce any vacuole formation. Cell damage with V_m of 0.67 V, which corresponded to a V_i of 10 V and R_e of 10 MΩ, is consistent with previous findings (1). Additional indications of cell viability include retention of dyes in the minutes following electroporation and cell motility after 2.5 h incubation.

Modified patch-clamp MEs apply pore-forming transmembrane potentials (0.2–1.0 V) with low electrode applied voltages (<10 V), because the electric fields are concentrated at the ME tip near the membrane. Use of low applied potentials makes automation by a computer possible because the maximum voltage from an A/D board is 10 V. Thus, aSCE offers a new and convenient method to noninvasively insert foreign molecules into adherent cells that is cell-specific and highly reproducible. Our new aSCE system, along with a new method to define the pulse amplitude, simplify SCE and provide enhanced tools to differentially manipulate the genetic, metabolic, fluorescent, and synthetic contents of single, targeted adherent cells in a population.

Acknowledgments

This work was supported in part by a grant to P.J.B. from the National Heart Lung and Blood Institute (R01 HL 077542-01A1), by a National Science Foundation Career Award to P.J.B. (BES 0238910), and by a seed grant from the Center for Optical Technologies, Bethlehem, PA.

References

1. Rae JL, Levis RA. Single-cell electroporation. Pflugers Arch. 2002; 443:664–670. [PubMed: 11907835]
2. Lundqvist JA, Sahlin F, Aberg MA, Stromberg A, Eriksson PS, Orwar O. Altering the biochemical state of individual cultured cells and organelles with ultramicroelectrodes. Proc Natl Acad Sci USA. 1998; 95:10356–10360. [PubMed: 9724707]
3. Nolkrantz K, Farre C, Brederlau A, Karlsson RI, Brennan C, Eriksson PS, Weber SG, Sandberg M, Orwar O. Electroporation of single cells and tissues with an electrolyte-filled capillary. Anal Chem. 2001; 73:4469–4477. [PubMed: 11575795]
4. Khine M, Lau A, Ionescu-Zanetti C, Seo J, Lee LP. A single cell electroporation chip. Lab Chip. 2005; 5:38–43. [PubMed: 15616738]

5. Needham D, Hochmuth RM. Electro-mechanical permeabilization of lipid vesicles. Role of membrane tension and compressibility. Biophys J. 1989; 55:1001–1009. [PubMed: 2720075]
6. Olofsson J, Nolkrantz K, Ryttsen F, Lambie BA, Weber SG, Orwar O. Single-cell electroporation. Curr Opin Biotechnol. 2003; 14:29–34. [PubMed: 12565999]
7. Teissie J, Rols MP. An experimental evaluation of the critical potential difference inducing cell membrane electropermeabilization. Biophys J. 1993; 65:409–413. [PubMed: 8369446]
8. Kinosita K Jr, Tsong TY. Voltage-induced conductance in human erythrocyte membranes. Biochim Biophys Acta. 1979; 554:479–497. [PubMed: 486454]
9. Weaver JC. Electroporation: a general phenomenon for manipulating cells and tissues. J Cell Biochem. 1993; 51:426–435. [PubMed: 8496245]
10. Frey W, White JA, Price RO, Blackmore PF, Joshi RP, Nuccitelli R, Beebe SJ, Schoenbach KH, Kolb JF. Plasma membrane voltage changes during nanosecond pulsed electric field exposure. Biophys J. 2006; 90:3608–3615. [PubMed: 16513782]
11. DeBruin KA, Krassowska W. Modeling electroporation in a single cell. I. Effects of field strength and rest potential. Biophys J. 1999; 77:1213–1224. [PubMed: 10465736]

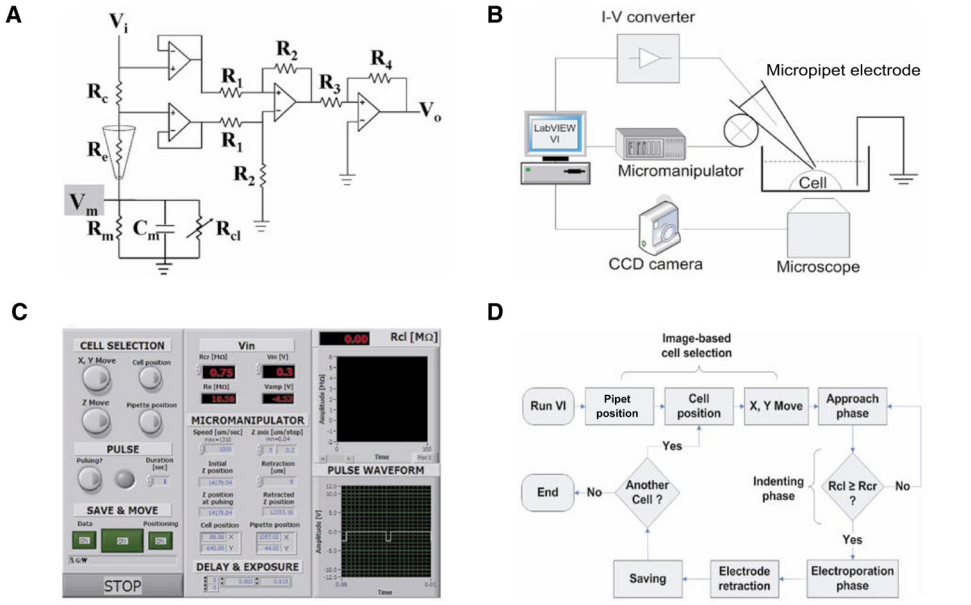

Figure 1. Components of automated single-cell electroporation (aSCE)

(A) Modified current-to-voltage (I–V) converter circuit. V_i, dc/pulse input voltage; V_o, output voltage; R_c, measurement resistance (100 kΩ); R_e, electrode resistance (10–20 MΩ); R_m, membrane resistance; C_m, membrane capacitance; R_{cl}, cleft resistance; R_1 and R_2, difference amplifier resistance (100 Ωand 1 kΩ, respectively); R_3 and R_4, amplifier resistance (10 and 470 Ω, respectively). (B) aSCE experimental setup. aSCE consists of micropipet electrode (ME), micromanipulator, charge-coupled device (CCD) camera, I–V converter, computer, and microscope. (C) Features and options in the graphic-user interface. V_m and R_{cr} are controllable, and options such as saving data and images, micromanipulator speed, camera exposure time, and retraction length are displayed on the front panel. (D) aSCE protocol. After image capture, a cell position for microelectroporation was selected by image-based cell selection. The ME (attached to computer-controlled motorized micromanipulator) was moved to the selected position (x- and y-axis movement). During approach phases, the electrode was moved incrementally in the z direction until it touched and indented the cell membrane (indenting phase). Approach was stopped when the cleft resistance reached the critical resistance value, R_{cl} (approximately 0.75 Ω). The electroporation phase was then initiated using preselected membrane voltage (V_m) (square-wave pulse frequency, 200 Hz; duration, 1 s; duty ratio, 10%), which induced membrane pore formation and the transport of molecules into the cell via electrophoresis and diffusion. Upon completion of electroporation, the ME was retracted, and data was saved.

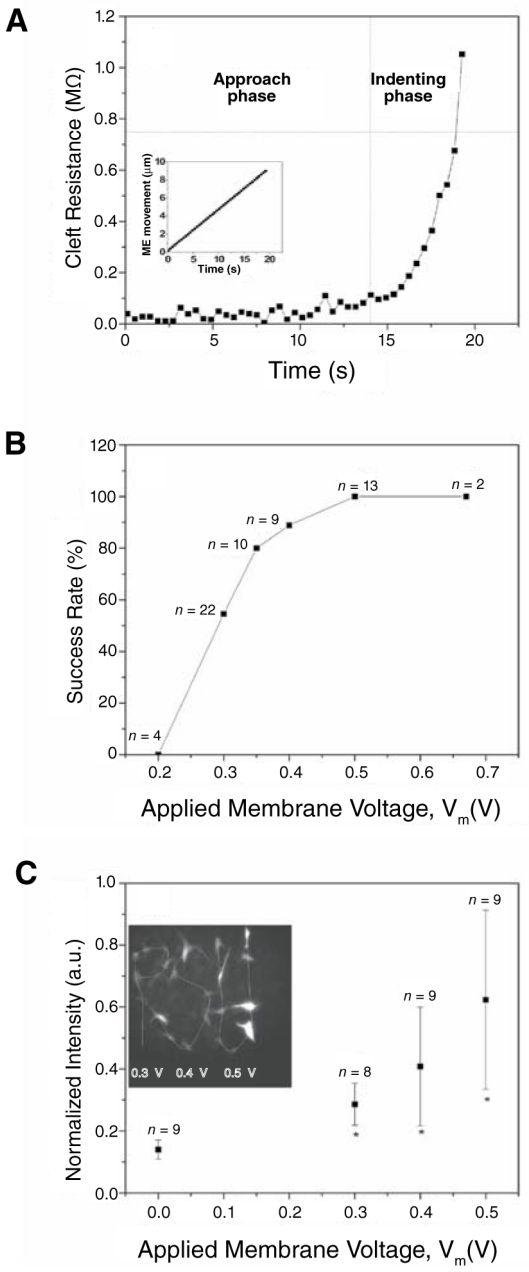

Figure 2. Electroporation degree and efficiency

(A) Cleft resistance (R_{cl}) versus time; R_{cl} was stable during approach phase, then sharply increased when micropipet electrode (ME) touched and indented the cell membrane. Indentation improves pipet sealing by the membrane. Horizontal dashed line indicates R_{cr}. Inset: ME movement as a function of time. (B) Electroporation success rate versus applied membrane voltage (V_m). Success was achieved when cell fluorescence was 2 sd above cellular intrinsic fluorescence; success ratio increased as V_m increased; 90% success rate was achieved with V_m = 0.4 V. (C) Inserted BODIPY FL-GTP intensity versus applied V_m; cells were selected individually using V_m of 0.3, 0.4, and 0.5 V for cells marked by P, S, and U, respectively. Inserted dye intensity was highly dependent on V_m. Cell viability was confirmed by calcein staining, phase microscopy, and absence of electroporation-induced

vesicles, dye leakage, or membrane bleb formation. * Indicates significant difference from average cell intrinsic fluorescence as determined by analysis of variance (ANOVA) and a Student's *t*-test ($P < 0.01$). a.u., arbitrary units.